

# Co-combustion and emission characteristics of coal gangue and low-quality coal

Yingyi Zhang · Jinichiro Nakano · Lili Liu ·  
Xidong Wang · Zuotai Zhang

Received: 2 September 2014 / Accepted: 22 January 2015 / Published online: 18 February 2015  
© Akadémiai Kiadó, Budapest, Hungary 2015

**Abstract** The reuse of coal gangue for energy recovery is developing rapidly in China, due to its advantage in achieving both economic and environmental benefits. Low-quality coal is often added to elevate the calorific value of the fuel. In this paper, the combustion characteristics as well as pollutant emissions ( $\text{SO}_2$  and  $\text{NO}$ ) of coal gangue, low-quality coal and their blends at different proportions were investigated by using both thermal analysis and fixed-bed reactor. Results showed that compared with pure coal gangue, co-combustion with low-quality coal lowered ignition and burnout temperature, but only slightly decreased the activation energy. In regard to pollution emissions, the coal addition contributed to the tailing peak of  $\text{SO}_2$  emission during co-combustion, which may influence the desulfurization process. The co-combustion elevated the  $\text{NO}$  yield due to high nitrogen content in the coal used. An increase in char content with increasing coal ratio in turn promoted a reduction in  $\text{NO}$ .

**Keywords** Coal gangue · Low-quality coal · Co-combustion · Kinetic · Emission

---

**Electronic supplementary material** The online version of this article (doi:[10.1007/s10973-015-4477-4](https://doi.org/10.1007/s10973-015-4477-4)) contains supplementary material, which is available to authorized users.

---

Y. Zhang · L. Liu · X. Wang · Z. Zhang (✉)  
Beijing Key Laboratory for Solid Waste Utilization and Management and Department of Energy and Resource Engineering, College of Engineering, Peking University, Beijing 100871, People's Republic of China  
e-mail: zuotaizhang@pku.edu.cn

J. Nakano  
URS Corp., PO BOX 1959, Albany, OR 97321, USA

## Introduction

Coal gangue is a problematic by-product generated from the process of mining and beneficiation of coal. It approximately accounts for 10–15 mass % of coal production [1]. Huge quantities of coal gangue has been stockpiled during decades of coal production and cause severe environmental impacts, such as acid drainage, heavy metals leaching as well as atmospheric pollution [2–4]. Since coal gangue usually has certain calorific heating values, it can be used for energy recovery, which is considered as an effective way to reduce the disposal cost and environmental hazards, and to bring economic benefits [5]. As the calorific value of coal gangue is low, it is usually co-combusted with coal. In China, the utilization of coal gangue or its blends with coal in energy recovery can receive subsidies from the government, if the total calorific value of the fuel is lower than  $12.56 \text{ MJ kg}^{-1}$ . The utilization of coal gangue as primary fuel for energy recovery was up to 140 million tons in 2011 in China [6].

The co-fire of coal with biomass, sewage sludge and municipal refuse has been attracting great interest recently [7–11]; however, the studies concerning the co-combustion of coal/coal gangue are limited. Compared with coal, coal gangue has high ash content and low carbon content. The combustion characteristics of coal gangue should be different from that of coal. Besides, the mineral species in coal and coal gangue may also be of great difference. These differences may influence the combustion behavior and efficiency of their blends. It is reported that the synergistic interactions taking place during the combustion of different fuels may influence the ignition and burn out behavior and cannot be estimated from the behavior of the individual ingredients [12–14]. Therefore, for the better development of the reuse of coal gangue for energy

recovery, it is crucial to carry out a systematical investigation on the combustion behavior of coal gangue and coal blends. Thermo-analytical analysis is one of the most commonly employed techniques to give a rapid assessment of the fuel [15]. The thermal behavior and characteristics parameter of the fuel, such as ignition and burnout temperature, maximum reactivity temperature as well as kinetics, can be obtained. This information can be used to predict the combustion behavior of the fuel on larger scale, allow accurate design of combustion facilities as well as control the process properly. Hence, a systematic thermal analysis of coal gangue and coal blend can make an important contribution for its application in practice.

On the other hand, a growing environmental awareness has resulted in increasingly stringent regulations on pollution emission. Both coal and coal gangue contain sulfur and nitrogen, which result in sulfur dioxide (SO<sub>2</sub>) and nitric oxides (NO<sub>x</sub>) emissions [16, 17]. The emission behavior of the blends of coal gangue and coal has not been reported. Sulfur in coal and coal gangue can exist in both organic and inorganic forms [18, 19]. Compared with coal, the content of organic sulfur in coal gangue is small. Nitrogen in coal/coal gangue majorly exists in an organic form. The emission of NO<sub>x</sub> is greatly influenced by the oxidation of volatile nitrogen and char nitrogen as well as the reduction reaction on the char surface. The different blending ratios of coal/coal gangue result in different proportions of volatile and char, which may influence the emission of NO<sub>x</sub>. For the sustainable development of coal gangue utilization, a systematic investigation regarding the pollution emission of coal gangue/coal blends is also needed.

In response to the booming development of coal gangue energy recovery coupled with the increasingly stringent emission regulations, it is important to gain better knowledge of both the combustion characteristics and pollution emission behaviors of coal gangue/coal blends. The present study was therefore motivated. In this work, the combustion behaviors of coal gangue, low-quality coal and their blends were studied using a thermogravimetric analysis with differential scanning calorimetry (TG-DSC) apparatus. The SO<sub>2</sub> and NO emissions during combustion of the fuels were investigated on a relatively large-scale tube furnace. The aim of this work was to give a comprehensive appraisal to the co-combustion of coal gangue and coal, and the results help to promote the development of coal gangue utilization for energy recovery.

## Experimental

### Materials

The coal gangue (denoted as CG) and coal samples were both acquired from Pingshuo coal gangue power generation

plant in Shanxi Province, China. The samples were milled and sieved to a grain size fraction of 150 μm. Proximate analysis was carried out by a thermogravimetric analyzer (TGA-701, LECO), and ultimate analysis was performed by an elemental analyzer (vario Macro CHNS, Elementar). The chemical compositions of the ash content were determined by an X-ray fluorescence spectrometer (S4-Explorer, Bruker). The calorific value was determined by adiabatic bomb calorimetry (Parr 6400 Calorimeter, Parr). In this study, coal was blended with coal gangue at mass ratios of 80:20, 70:30 and 60:40, respectively. To ensure the homogeneity of each fuel blend, the powder components were thoroughly mixed in an agate mortar before analysis.

### Methods

#### *Fourier transform infrared spectroscopy analysis (FTIR)*

Fourier transform infrared spectroscopy analysis (VECTOR22, Bruker) was conducted to investigate the structure of coal gangue and coal. About 2 mg of sample was co-grounded with 200 mg KBr in an agate mortar and pressed to a 13.0-mm-diameter disk for the measurements. The spectra were recorded in the range of 4,000–400 cm<sup>-1</sup> at a resolution of 2 cm<sup>-1</sup>, and co-adding of 64 scans was chosen.

#### *Thermal analysis*

The TG, derivative thermogravimetric (DTG) and DSC analysis of coal gangue, coal and their blends were carried out using a thermal analyzer (Q600SDT, TA Instruments). Approximately 10 mg of sample was employed in each experiment and flatly dispersed in the alumina crucible. A blank alumina crucible was employed as reference. The analyses were performed under air atmosphere at constant flow rate of 100 mL min<sup>-1</sup>. Four linear heating rates of 10, 20, 30 and 40 °C min<sup>-1</sup> were chosen, and the temperature ramped from room temperature to 1,000 °C. Repeat experiments under one testing condition were conducted three times to examine the reproducibility of the results. In repeat experiments, 10 mg coal gangue was used and the thermogravimetric experiments were conducted under a heating rate of 20 °C min<sup>-1</sup>. The results of repeat experiments are shown in Fig. S11 in supporting information. It can be seen that the TG curves superposed well and the fluctuation was acceptable.

#### *Pollution emissions experiments*

The samples were combusted in a fixed-bed reactor system. The system majorly consists of a vertical corundum tube

furnace. The furnace is electrically heated, and the temperature is measured by a thermocouple. The outlet of the furnace is connected to a flue gas analyzer (Testo pro350, Testo) by which the release of SO<sub>2</sub> and NO was measured simultaneously every 2 s. The furnace was first heated up and maintained at 850 °C. Then, the samples were quickly fed into the furnace. For each run, 250 mg of sample was finely dispersed in a thin layer in corundum crucible which has a depth of 1 cm and a diameter of 6 cm to improve the gas–solid contact. The air (purity >99 %, provided by Qianxi gas company, Beijing, China, Ltd.) supply to the furnace was kept at a constant flow rate of 1.2 L min<sup>-1</sup>.

#### X-ray differential analysis (XRD)

The crystalline mineral phases of coal gangue, coal and the residue ash after combustion tests were identified by means of a rotary anode X-ray powder diffractometer (D/MAX-PC 2500, Rigaku). The diffractometer is equipped with a Cu-target tube, graphite monochromator and Ni filter. The Cu K $\alpha$  radiation ( $\lambda = 0.15406$  nm) was generated at a voltage of 40 kV and current of 100 mA. The continuous scan mode was used, and the scan range of  $2\theta$  was over 10–70° with an increment of 0.02°, under the scan speed of 4° min<sup>-1</sup>. The samples were prepared as random pressed powder, and the measurements were conducted at room temperature.

## Results and discussions

### Characteristics of coal gangue and coal

The proximate and ultimate analyses results of coal gangue and coal are presented in Table 1. It can be seen that compared with coal, coal gangue yields relatively high ash content, low volatile and fixed carbon content. The elemental content of nitrogen in coal gangue is lower than that in coal, while sulfur in coal gangue is relatively higher than that in coal. The analyses of the ash composition show that coal gangue and coal have similar ash compositions. The XRD patterns of coal gangue and coal are shown in Fig. 1. It can be seen that the diffraction peaks of coal gangue are more distinctive and stronger than that of coal. Compared with coal gangue, the hump on XRD patterns of coal can be clearly observed due to its high content of amorphous carbon. Despite the structural difference, the coal gangue and coal samples used in the present study showed similar mineral components: majorly kaolinite and quartz. Minor amounts of pyrite and calcite were also observed in coal gangue and coal, respectively. Since the coal gangue and coal samples employed were generated from the same geological origin, it may result in the similarity in ash compositions. The FTIR spectra of coal gangue and coal

**Table 1** Chemical compositions of coal gangue and coal

	CG	Coal
<i>Proximate analysis/mass %</i>		
Moisture, ad	1.27	3.79
Ash, d	64.96	21.47
Volatile matter, d	16.36	31.61
Fixed carbon, d	18.68	45.93
<i>Ultimate analysis/mass %</i>		
C, ad	20.37	60.58
H, ad	2.14	1.41
N, ad	0.60	1.29
S, ad	2.36	1.64
Calorific values/MJ kg <sup>-1</sup>	6.47	24.21
<i>Ash composition/mass %</i>		
SiO <sub>2</sub>	49.7	47.9
Al <sub>2</sub> O <sub>3</sub>	43.9	42.8
Fe <sub>2</sub> O <sub>3</sub>	2.11	4.68
CaO	0.21	2.13
MgO	0.11	0.59
K <sub>2</sub> O	0.18	0.33
Na <sub>2</sub> O	<0.1	0.14
TiO <sub>2</sub>	1.50	1.17

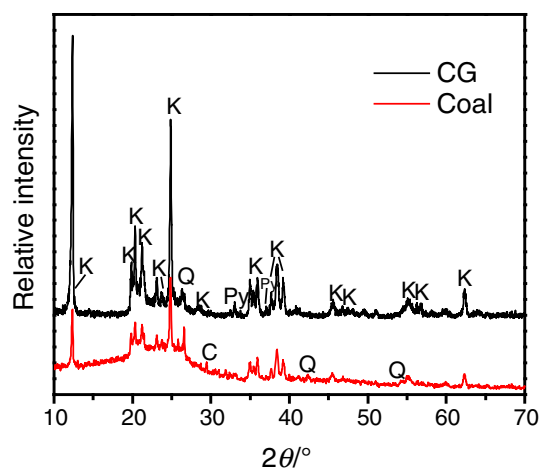


**Fig. 1** XRD patterns of coal gangue and coal. K-kaolinite (Al<sub>2</sub>Si<sub>2</sub>O<sub>5</sub>(OH)<sub>4</sub>), Q-quartz (SiO<sub>2</sub>), C-calcite (CaCO<sub>3</sub>), Py-pyrite(FeS<sub>2</sub>)

(shown in Fig. 2) may help further understanding their difference in structure. The assignments of the bands are also labeled in Fig. 2. It can be seen that coal revealed well-developed carbon-related bands in the range of 3,000–2,600 cm<sup>-1</sup> as well as 1,800–1,200 cm<sup>-1</sup>. On the contrary, coal gangue presented strong ash-related bands at 1,200–400 cm<sup>-1</sup> due to its high ash content. The difference in their structure may lead to the difference of their combustibility.

## Co-combustion behavior of coal gangue, coal and the blends

### Co-combustion characteristics

The TG, DTG and DSC profiles of coal gangue, coal and their blends under temperature programmed combustion obtained at heating rate of  $10\text{ }^{\circ}\text{C min}^{-1}$  are shown in Fig. 3. The influence of heating rates on TG, DTG and DSC curves is shown in Fig. SI2 in supporting information, taking sample Coal 30 % as example. It can be seen from Fig. 3 that the combustion process of coal gangue and coal can both be divided into four representative regimes for interpreting. From ambient temperature to  $100\text{ }^{\circ}\text{C}$ , corresponds to the evaporation of moisture, i.e., surface water, bound water and void water [20]. From  $100$  to  $300\text{ }^{\circ}\text{C}$ , the mass was inconspicuously gained, which was noticeable for coal, probably due to the oxygen chemisorptions of carbon and volatile matter [20]. The tiny mass gain indicated the onset of the organic matter combustion. The combustion process took place at  $300\text{--}700\text{ }^{\circ}\text{C}$ , which was manifested by a major mass loss on the TG profiles for coal and coal gangue. It can be seen from the DTG profiles that a shoulder slope appears at the beginning of the major overlapping peak for both coal and coal gangue at  $300\text{--}400\text{ }^{\circ}\text{C}$ . The DSC curves further clearly showed a peak in the same temperature range. It indicated that the combustion process was composed of two steps: the combustion of volatile matter in the interval of  $300\text{--}400\text{ }^{\circ}\text{C}$  and the combustion of residual char in the interval of  $400\text{--}700\text{ }^{\circ}\text{C}$  [21].

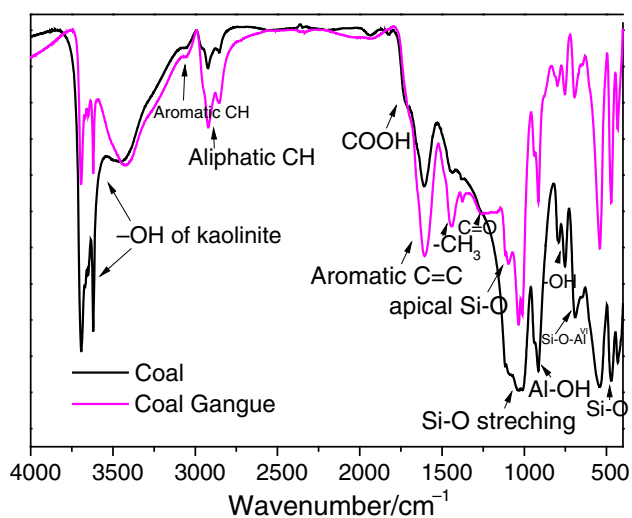


**Fig. 2** FTIR spectra of coal gangue and coal

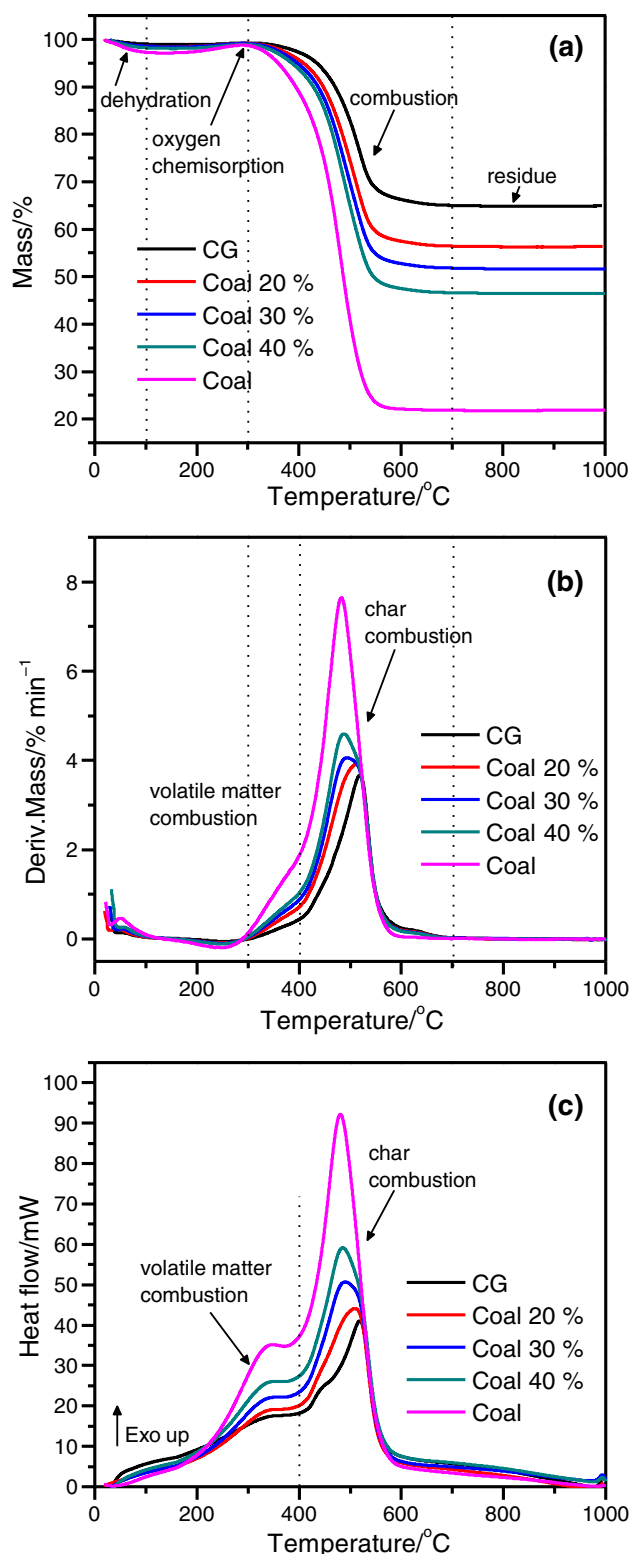


**Fig. 3** Thermogravimetric (TG), derivative thermogravimetric (DTG) and differential scanning calorimetric (DSC) curves of coal gangue, coal and their blends. The upward peaks on DSC curves represent exothermic reaction

The characteristic parameters of the combustion process of coal, coal gangue and their blends at heating rate of  $10\text{ }^{\circ}\text{C min}^{-1}$  are presented in Table 2. As coal has more content of volatile matter as well as fixed carbon, the mass loss rate of coal was significantly higher than that of coal gangue. So was the exothermic peak area. It was also noticed that both the ignition temperature and burnout temperature of coal was lower than that of coal gangue. Therefore, with the co-combustion of coal, the combustion properties of coal gangue may be elevated in lower ignition temperature, higher reactivity and better burnout performance. The thermal behaviors of the blends in Fig. 3 show that the combustion properties of blends are more similar to that of coal gangue. With the increase of coal content in fuel blends, the ignition temperature and DTG peak temperature become lower and its corresponding mass loss rate becomes higher. On the other hand, the change in burnout temperatures of blends with different coal ratio is not significant. Compared with other waste materials, coal gangue and coal show similar thermal behavior in general. It should be attributed to the similar chemical compositions of coal gangue and coal. The same geological origin of the samples used in the present study also contributes to the similar combustion temperature range. As a consequence, the furnace problems related to differences between fuels may be largely reduced.

### Kinetics

The reaction rate of heterogeneous solid-state reactions can be generally described by

$$\frac{d\alpha}{dt} = Ae^{-E/RT}f(\alpha) \quad (1)$$

where  $\alpha$  is the conversion degree,  $A$  is the pre-exponential Arrhenius factor,  $E$  is the activation energy,  $R$  is the gas constant, and  $f(\alpha)$  is the reaction model.

For a constant heating rate  $\beta$ ,  $\beta = dT/dt$ , an integral form of the reaction model  $g(\alpha)$  can be expressed as:

$$\int_0^{\alpha} \frac{d\alpha}{f(\alpha)} = g(\alpha) = \frac{A}{\beta} \int_{T_0}^T e^{-E/RT} dT \quad (2)$$

The iso-conversional method by Flynn–Wall–Ozawa is used for the estimation of the apparent activation energy ( $E_a$ ). The iso-conversional method allows the calculation of the activation energy without prior knowledge on mechanism function. Therefore, it provides relatively reliable insights into the kinetics of complex reaction processes. The equation of Flynn–Wall–Ozawa method is expressed as [22–26],

$$\ln \beta = \ln \left[ \frac{AE}{g(\alpha)R} \right] - 5.331 - 1.052 \frac{E}{RT} \quad (3)$$

The conversion degree  $\alpha$  can be derived from TG/DTG curves of the fuel as follows:

$$\alpha = \frac{m_0 - m_t}{m_0 - m_{\infty}} \quad (4)$$

where  $m_0$ ,  $m_t$  and  $m_{\infty}$  are the mass of coal gangue at initial, a time  $t$  and after the reaction, respectively. For different  $\alpha$ , the  $E_a$  was calculated from the slope of lines by plotting  $\ln \beta$  versus  $1/T$ .

The plots of  $\ln \beta$  versus  $1/T$  for coal gangue, coal and their blends at different conversion ratios are shown in Fig. 4. The activation energy values and the corresponding correlation coefficient  $R^2$  for coal gangue, coal and their blends at different conversion ratios are presented in Table 3. It can be seen that the activation energies for all the fuels had high  $R^2$  values, which manifested the acceptable accuracy of the results. The activation energy of coal gangue is significantly higher than that of coal. As the conversion ratio increases, the activation energy shows a declining trend in general. The activation energy of coal decreases more sharply than that of coal gangue and the blends. The decrease in activation energy indicates that less energy is required as combustion proceeds. As the combustion proceeds, the temperature increases and less carbon matter is left with more porous structure. Therefore, less energy is needed. Coal has more carbon structure, as can be seen from FTIR spectra (Fig. 2). It is easier to ignite and has larger exothermal effect. Therefore, the activation energy of coal is lower and decreases more sharply than coal gangue as well as the blends. For samples Coal 30 % and Coal 40 %, the activation energy slightly increases at 0.1–0.4 conversion ratio. The slight increase in

**Table 2** Characteristic parameters of combustion process of coal, coal gangue and their blends

Sample	Ignition $T_i/^{\circ}\text{C}$	DTG peak $T_{\max}/^{\circ}\text{C}$	DTG <sub>max</sub> $R_{\max}/\text{mg } ^{\circ}\text{C}^{-1}$	DSC peak $T_{\max}/^{\circ}\text{C}$	Burn out $T_f/^{\circ}\text{C}$
CG	457	519	0.37	520	552
Coal 20 %	435	512	0.39	510	545
Coal 30 %	426	493	0.41	490	542
Coal 40 %	424	487	0.46	485	539
Coal	421	482	0.76	480	523

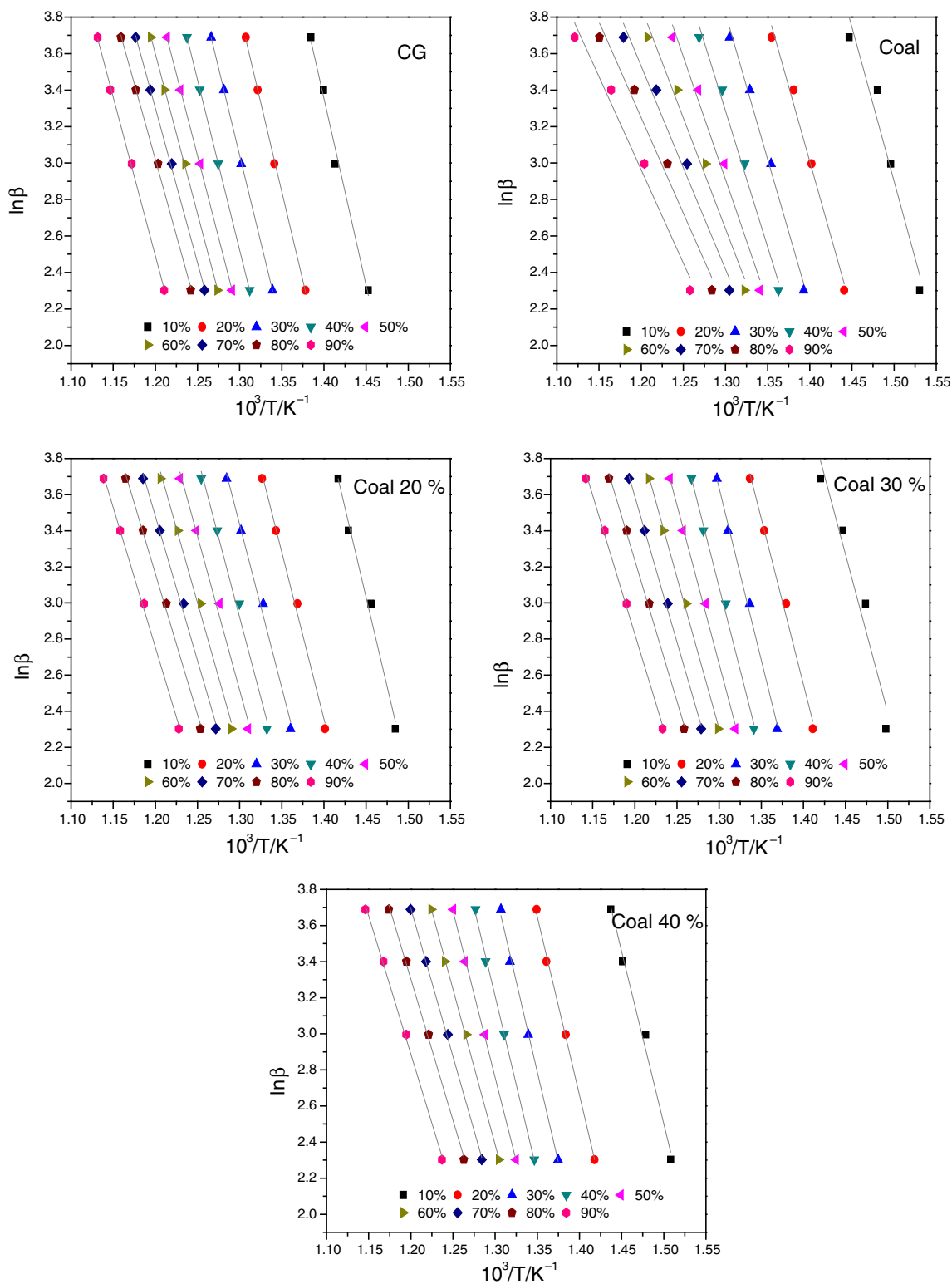


**Fig. 4** Plots for the determination of activation energy at different conversion ratios corresponding to the combustion of coal gangue (CG), coal and their blends (Coal20 %, Coal30 % and Coal 40 %)

activation energy should be ascribed to the oxidative pyrolysis process [27]. It may be due to that the increase in coal addition results in incomplete combustion of the fuel blends

at the beginning. However, it seems that the addition of coal has a limited effect on lowering the activation energy of the fuel blends.



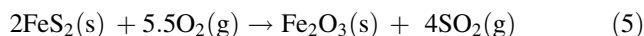
**Table 3** Activation energy of coal gangue, coal and their blends

Sample	$\alpha$	$E/kJ\ mol^{-1}$	$R^2$
CG	0.1	162	0.98528
	0.2	154	0.99919
	0.3	151	0.99968
	0.4	147	0.99998
	0.5	142	0.99971
	0.6	138	0.99936
	0.7	134	0.99896
	0.8	132	0.99808
	0.9	137	0.99889
Coal 20 %	0.1	156	0.98579
	0.2	146	0.99282
	0.3	143	0.9904
	0.4	140	0.98802
	0.5	135	0.98864
	0.6	130	0.9914
	0.7	126	0.99416
	0.8	124	0.99587
	0.9	123	0.99761
Coal 30 %	0.1	138	0.92705
	0.2	145	0.98918
	0.3	150	0.99385
	0.4	145	0.99395
	0.5	146	0.99504
	0.6	139	0.9965
	0.7	133	0.99754
	0.8	127	0.9971
	0.9	122	0.997
Coal 40 %	0.1	151	0.9864
	0.2	157	0.99711
	0.3	159	0.99662
	0.4	155	0.99815
	0.5	146	0.99896
	0.6	136	0.99904
	0.7	130	0.99895
	0.8	124	0.99776
	0.9	121	0.99752
Coal	0.1	134	0.93405
	0.2	130	0.98387
	0.3	126	0.98962
	0.4	118	0.98325
	0.5	106	0.97822
	0.6	96	0.97354
	0.7	88	0.97249
	0.8	83	0.97152
	0.9	81	0.96937

SO<sub>2</sub> and NO emission of coal gangue, coal and the blends

SO<sub>2</sub> emission

SO<sub>2</sub> and NO<sub>x</sub> emissions are the major environmental concern associated with the combustion process of fossil fuel. The SO<sub>2</sub> emission profiles of coal gangue, coal and their blends at 850 °C are illustrated in Fig. 5. It can be seen from Fig. 5 that the SO<sub>2</sub> emission profiles of coal gangue and coal are quite different. Sulfur in coal gangue majorly exists in form of pyrite. Therefore, the formation of SO<sub>2</sub> during combustion of coal gangue is mainly governed by the oxidation of pyrite. As for coal, the situation may become more complicated. Sulfur in coal may be present as organic, inorganic and elemental sulfur [28]. It can be seen that the SO<sub>2</sub> emission of coal gangue shows a single sharp peak, while that of coal shows a mild peak with a shoulder peak at the beginning and a long tailing peak. It may have resulted from the different occurrence of sulfur in the fuel. Another possible reason is the different transformation behavior of the embedded pyrite. The chemical structure and content of combustible matters are largely different in coal gangue and coal. It may cause the difference in local temperature, structure and gas compositions of the embedded pyrite, which eventually affects its transformation behavior and SO<sub>2</sub> emission behavior. In oxygen-containing atmosphere, the major overall transformation process of pyrite is listed below [29, 30]:



In addition, the ferrous sulfate and ferric sulfate may also form according to the following reactions (majorly Eq. 6):

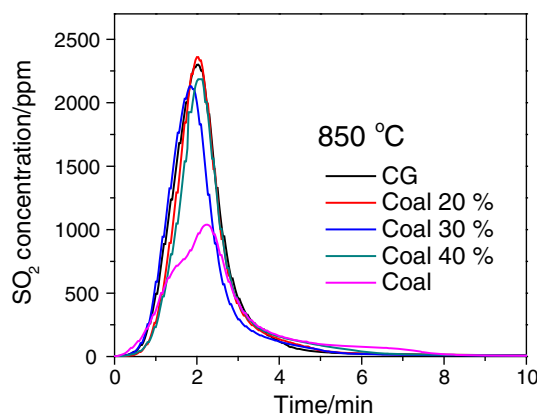
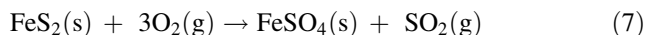
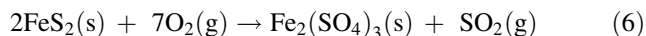


**Fig. 5** SO<sub>2</sub> emission profiles of coal gangue, coal and their blends at 850 °C



Compared with coal gangue, coal contains less mineral content. Therefore, during combustion, the embedded pyrite is more likely to expose directly to the oxygen, which favors the formation of ferric sulfate. Due to the large molar volume of ferric sulfate, it may behave like a shell over the unreacted pyrite core and partially block the diffusion of oxygen, which therefore result in the tailing peak on the  $\text{SO}_2$  emission profile. The  $\text{SO}_2$  emission profiles of the blends are similar to that of coal gangue, which may be attributed to the large contribution of sulfur content from coal gangue. With the increase in coal ratio, the tailing peak can be observed. The appearance of the tailing peak on  $\text{SO}_2$  emission indicates longer emission time of  $\text{SO}_2$ , which may influence the desulfurization efficiency in practice.

### NO emission

The NO emission profiles of coal gangue, coal and their blends at 850 °C are illustrated in Fig. 6a. For both coal gangue and coal, two peaks can be observed on NO emission profiles. During combustion process, the NO emission is majorly contributed by the fuel-N conversion [31]. Since the fuel-N is distributed in both volatile matters and solid char matrix, the two emission peaks are corresponding to the formation of NO during volatile matter combustion and residual char combustion, respectively. It can be seen from Fig. 6a that the NO emission profiles of coal gangue and coal are largely different. Since coal contains more volatile matter and fixed carbon than coal gangue, the volatile NO peak of coal is strong, while that of coal gangue is weak. It is found that the peak value of char NO of coal is lower than that of coal gangue. According to the ultimate analyses, the nitrogen content in coal is twice that of coal gangue. The lower in peak value may be due to the stronger reduction of NO on the surface of well-developed char structure of coal.

The total NO yields of coal gangue, coal and their blends are present in Fig. 6b. The total amount of NO yield of coal is almost twice that of coal gangue, which is in accordance with their nitrogen contents. Compared with pure coal gangue, the co-combustion with coal is found to elevate in the NO yield, which may pose challenge to its application. With the increase in coal ratio from 20 to 30 mass %, the generation of NO slightly increases. When the coal ratio increases to 40 mass %, further increase in total NO yield, however, is not observed. The suggested reason is that the increase in coal ratio provides more char during combustion process, which in turn promotes the reduction in NO.

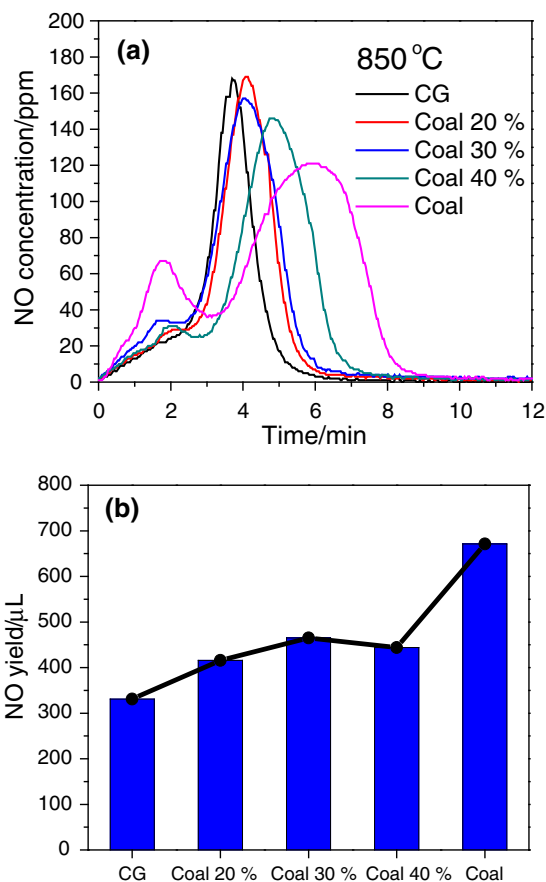


**Fig. 6** NO emission profiles and total yield of coal gangue, coal and their blends at 850 °C

### Characteristics of residue ash

The XRD patterns of residual ash of coal gangue, coal and their blends after combustion at 850 °C are shown in Fig. 7. A significant amorphous peak can be observed on the diffraction patterns for all the residue ash. Since both coal gangue and coal contain significant amount of kaolinite, the notable amorphous peak in residual ash belongs to the semi-crystalline metakaolinite generated after dehydroxylation of kaolinite. As the combustion temperature is relatively low, the further transformation of metakaolinite to mullite is prohibited. As a consequence, the residual ash would possess sufficient reactivity under appropriate conditions since it contains the significant amount of non-crystalline phase. Thus, the residual ash may have good application in construction materials manufacture, such as cement, concrete or geopolymer.

Besides, hematite can be found in all the patterns, which is due to the oxidation of pyrite (Eq. 5). Magnetite is also observed in the residue ash of coal, which may be ascribed to the complex transformation behavior of embedded pyrite [30]. This may also manifest that due to different chemical



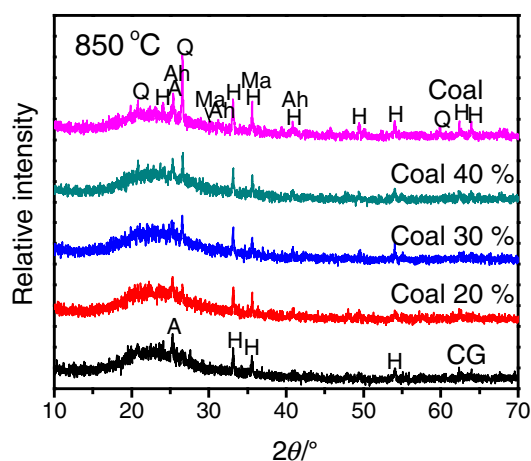
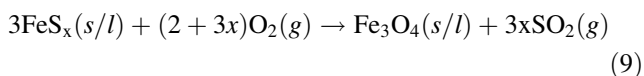
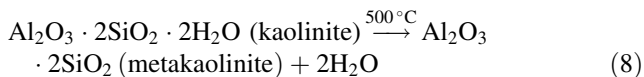


**Fig. 7** XRD patterns of the residual ash of coal gangue, coal and the blends after combustion at 850 °C. A-anatase (TiO<sub>2</sub>), H-hematite (Fe<sub>2</sub>O<sub>3</sub>), Q-quartz (SiO<sub>2</sub>), Ah-anhydrite (CaSO<sub>4</sub>) and Ma-magnetite (Fe<sub>3</sub>O<sub>4</sub>)

compositions of coal gangue and coal, the transformation behaviors of embedded pyrite would be different. For the coal has certain content of calcite (shown in Fig. 1), the lime generated due to decomposition of calcite can react with sulfur dioxide, which results in the formation of anhydrite in residue ash of coal. Quartz and anatase, which are obtained from the raw materials, remain stable. The involved reactions are shown as follows.



## Conclusions

The combustion of coal gangue, coal and their blends at different proportions was systematically investigated in regarding to the combustion characteristics and pollution emission. Compared with coal, coal gangue has low volatile matter, low fixed carbon and high ash content. It was found that the co-combustion with coal can improve the combustion performance of coal gangue in lower ignition temperature and burnout temperature, but can only slightly decrease the activation energy. In the respect of pollution emission, compared with pure coal gangue combustion, the

co-fire with coal has limited effect on SO<sub>2</sub> emission, except the contribution to the tailing peak. It may influence the desulfurization process in practice. As coal contains higher nitrogen content than coal gangue, the co-combustion of blending fuel elevates the NO yield. Meanwhile, it is noticed that the increase in char content with increasing coal ratio in turn promotes the reduction in NO, which limits the elevation of NO yield with increasing coal content.

**Acknowledgements** The authors gratefully acknowledge financial support by the Common Development Fund of Beijing and the National Natural Science Foundation of China (51172001, 51172003 and 51272005). Supports by the National High Technology Research and Development Program of China (863 Program, 2012 AA06A114) and Key Projects in the National Science and Technology Pillar Program (2013 BAC14B07 and 2011 BAB03B02) are also acknowledged.

## References

- Liu HB, Liu ZL. Recycling utilization patterns of coal mining waste in China. *Resour Conserv Recycl.* 2010;54(12):1331–40.
- Zhao YC, Zhang JY, Chou CL, Li Y, Wang ZH, Ge YT, Zheng CG. Trace element emissions from spontaneous combustion of gob piles in coal mines, Shanxi, China. *Int J Coal Geol.* 2008;73(1):52–62.
- Nichol D, Tovey NP. Remediation and monitoring of a burning coal refuse bank affecting the Southsea Looproad at Brymbo, North Wales. *Eng Geol.* 1998;50(3–4):309–18. doi:10.1016/S0013-7952(98)00030-1.
- Ardejani FD, Shokri BJ, Bagheri M, Soleimani E. Investigation of pyrite oxidation and acid mine drainage characterization associated with Razi active coal mine and coal washing waste dumps in the Azad shahr-Ramian region, northeast Iran. *Environ Earth Sci.* 2010;61(8):1547–60.
- Meng FR, Yu JL, Tahmasebi A, Han YN. Pyrolysis and combustion behavior of coal gangue in O-2/CO<sub>2</sub> and O-2/N<sub>2</sub> mixtures using thermogravimetric analysis and a drop tube furnace. *Energy Fuel.* 2013;27(6):2923–32.
- The China Resources Utilization Annual Report (2012). [http://hzs.ndrc.gov.cn/newgzdt/201304/t20130412\\_536759.html](http://hzs.ndrc.gov.cn/newgzdt/201304/t20130412_536759.html).
- Xiao HM, Ma XQ, Liu K. Co-combustion kinetics of sewage sludge with coal and coal gangue under different atmospheres. *Energy Convers Manag.* 2010;51(10):1976–80.
- Zhou CC, Liu GJ, Cheng SW, Fang T, Lam PKS. Thermochemical and trace element behavior of coal gangue, agricultural biomass and their blends during co-combustion. *Bioresour Technol.* 2014;166:243–51.
- Xiao HM, Ma XQ, Lai ZY. Isoconversional kinetic analysis of co-combustion of sewage sludge with straw and coal. *Appl Energy.* 2009;86(9):1741–5.
- Liu Z, Zhang YS, Zhong LC, Orndroff W, Zhao HY, Cao Y, Zhang K, Pan WP. Synergistic effects of mineral matter on the combustion of coal blended with biomass. *J Therm Anal Calorim.* 2013;113(2):489–96.
- Yi QG, Qi FJ, Cheng G, Zhang YG, Xiao B, Hu ZQ, Liu SM, Cai HY, Xu S. Thermogravimetric analysis of co-combustion of biomass and biochar. *J Therm Anal Calorim.* 2013;112(3):1475–9.

12. Backreedy RI, Jones JM, Ma L, Pourkashanian M, Williams A, Arenillas A, Arias B, Pis JJ, Rubiera F. Prediction of unburned carbon and NO<sub>x</sub> in a tangentially fired power station using single coals and blends. *Fuel*. 2005;84(17):2196–203.
13. Haykiri-Acma H, Yaman S, Kucukbayrak S. Co-combustion of low rank coal/waste biomass blends using dry air or oxygen. *Appl Therm Eng*. 2013;50(1):251–9.
14. Faundez J, Arias B, Rubiera F, Arenillas A, Garcia X, Gordon AL, Pis JJ. Ignition characteristics of coal blends in an entrained flow furnace. *Fuel*. 2007;86(14):2076–80.
15. Jia CX, Wang Q, Ge JX, Xu XF. Pyrolysis and combustion model of oil sands from non-isothermal thermogravimetric analysis data. *J Therm Anal Calorim*. 2014;116(2):1073–81.
16. Lei M, Wang CB, Wang SL. Effect of pyrolysis characteristics on ignition mechanism and NO emission of pulverized coal during oxy-fuel combustion. *J Therm Anal Calorim*. 2014;117(2):665–73.
17. Cheng HF, Liu QF, Zhang S, Wang SQ, Frost RL. Evolved gas analysis of coal-derived pyrite/marcasite. *J Therm Anal Calorim*. 2014;116(2):887–94.
18. Querol X, Izquierdo M, Monfort E, Alvarez E, Font O, Moreno T, Alastuey A, Zhuang X, Lu W, Wang Y. Environmental characterization of burnt coal gangue banks at Yangquan, Shanxi Province, China. *Int J Coal Geol*. 2008;75(2):93–104.
19. Sun YZ, Fan JS, Qin P, Niu HY. Pollution extents of organic substances from a coal gangue dump of Jiulong coal mine, China. *Environ Geochem Health*. 2009;31(1):81–9.
20. Zhou CC, Liu GJ, Yan ZC, Fang T, Wang RW. Transformation behavior of mineral composition and trace elements during coal gangue combustion. *Fuel*. 2012;97:644–50. doi:[10.1016/j.fuel.2012.02.027](https://doi.org/10.1016/j.fuel.2012.02.027).
21. Chen Y, Mori S, Pan WP. Studying the mechanisms of ignition of coal particles by TG-DTA. *Thermochim Acta*. 1996;275(1):149–58.
22. Tahmasebi A, Kassim MA, Yu JL, Bhattacharya S. Thermogravimetric study of the combustion of *Tetraselmis suecica* microalgae and its blend with a Victorian brown coal in O<sub>2</sub>/N<sub>2</sub> and O<sub>2</sub>/CO<sub>2</sub> atmospheres. *Bioresour Technol*. 2013;150:15–27.
23. Otero M, Calvo LF, Gil MV, Garcia AI, Moran A. Co-combustion of different sewage sludge and coal: a non-isothermal thermogravimetric kinetic analysis. *Bioresour Technol*. 2008;99(14):6311–9.
24. Doyle C. Estimating isothermal life from thermogravimetric data. *J Appl Polym Sci*. 1962;6(24):639–42.
25. Flynn JH, Wall LA. General treatment of the thermogravimetry of polymers. *J Res Nat Bur Stand*. 1966;70(6):487–523.
26. Ozawa T. Estimation of activation energy by isoconversion methods. *Thermochim Acta*. 1992;203:159–65.
27. Idris SS, Rahman NA, Ismail K. Combustion characteristics of Malaysian oil palm biomass, sub-bituminous coal and their respective blends via thermogravimetric analysis (TGA). *Bioresour Technol*. 2012;123:581–91.
28. Chen LG, Bhattacharya S. Sulfur emission from victorian brown coal under pyrolysis, oxy-fuel combustion and gasification conditions. *Environ Sci Technol*. 2013;47(3):1729–34.
29. Paulik F, Paulik J, Arnold M. Kinetics and mechanism of the decomposition of pyrite under conventional and quasi-isothermal quasi-isobaric thermoanalytical conditions. *J Therm Anal*. 1982;25(2):313–25.
30. Hu GL, Dam-Johansen K, Stig W, Hansen JP. Decomposition and oxidation of pyrite. *Prog Energy Combust*. 2006;32(3):295–314.
31. Glarborg P, Jensen AD, Johnsson JE. Fuel nitrogen conversion in solid fuel fired systems. *Prog Energy Combust*. 2003;29(2):89–113.